arXiv:1302.0959v1 [nucl-th] 5 Feb 2013

Shell evolution of N=20 nuclei and Gamow-Teller strengths of ^{30,32,34}Mg by the deformed QRPA

Eunja Ha * and Myung-Ki Cheoun †
Department of Physics, Soongsil University, Seoul 156-743, Korea

(Dated: February 6, 2013)

Gamow-Teller (GT) strength distributions of Mg isotopes are investigated within a framework of the deformed quasi-particle random phase approximation(DQRPA). We found that the N=20 shell closure in $^{28\sim34}$Mg was broken by the prolate shape deformation originating from the *fp*-intruder states. The shell closure breaking gives rise to a shift of low-lying GT excited states into high-lying states. Discussions regarding the shell evolution trend of single particle states around N=20 nuclei are also presented with the comparison to other approaches.

PACS numbers: **23.40.Hc, 21.60.Jz, 26.50.+x**
Keywords:

The structure of nuclei along the valley of stability is well understood in terms of the conventional magic numbers in the nuclear shell model. In a region far from the stability, experimental studies have shown the breaking of the N=20 magic number in N=20 nuclei, such as ^{31}Na, ^{32}Mg, and ^{33}Al nuclei located in so called the island of inversion [1–3]. The breaking comes from the burrowing of $f_{7/2}$ and $p_{3/2}$ states below $d_{3/2}$ state [4], which may originate from the monopole component of the nucleon-nucleon interaction by the tensor force [5]. The breaking of magic numbers in the inversion island is thought as one of the interesting properties of the exotic nuclei near drip line.

The neutron-rich nuclei around N=20 are thought to be strongly deformed because of the reduction of the N=20 shell gap. The deformation in nuclei becomes more important than any other periods with the recent development of rare isotope accelerator facilities, from which one may perform lots of challenging experiments related to the exotic nuclei. Although they decay fractions of a second, their existence is imprinted on the nuclear abundances of stars through the successive nuclear reactions in the cosmos at the explosive stage of stellar evolution, such as supernovae (SNe) explosion [6].

For example, the nuclear reactions induced by the neutrinos emitted from the SNe are treated as important input data for the neutrino(ν)-process [7–9]. Since the neutrinos emitted from a proto-neutron star may have tens of MeV energy high enough to excite the deformed nuclei, one needs to understand more precisely the high-lying (HL) excited states beyond one nucleon threshold. Among them, the GT states are of great importance because most of the charge exchange reactions (CEXRs) are dominated by the GT transition. These HL GT excited states are in close association with the nuclear structure.

One of typical instances is the GT quenching problem. It says that the difference of total running sums $S_\pm$ for GT ($\pm$) transitions, $(S_- - S_+)$, is usually quenched compared to the Ikeda sum rule (ISR), $(S_- - S_+) = 3(N-Z)$. But, recent experimental data on HL GT states deduced by more energetic projectiles shed a new light on the GT states located above one nucleon threshold, whose contributions enable us to explain the quenching problem through the multi-particle and multi-hole configuration mixing [10].

Conventional approach to understand the nuclear structure is based on the spherical symmetry. But, in order to describe neutron-rich nuclei and their relevant nuclear reactions occurred in the nuclear processes, one needs to develop theoretical frameworks including explicitly the deformation [11, 12]. Ref. [11] used an effective separable force to the deformed quasi-particle random phase approximation (DQRPA). Realistic two-body interaction was firstly exploited at Ref. [12], but only with neutron-neutron (nn) and proton-proton (pp) pairing correlations which have only isospin T = 1 and J = 0 interaction. But, to properly describe the deformed nuclei, the T= 0 and J = 1 pairing should be also taken into account because the J = 1 pairing is believed as one of the reasons leading to the nuclear deformation.

In this paper, we apply our previous DQRPA [13, 14] to the nuclei in the N=20 inversion island. Starting from the deformed Wood Saxon potential [15], we transform a physical state given by the diagonalization of total Hamiltonian in the Nilsson basis into the spherical basis, in which one can perform more easily theoretical calculations. Then deformed BCS equation can be solved by using *ab initio* Brueckner G-matrix represented in the deformed basis for the nucleon-nucleon interaction inside nuclei as follows.

With the expansion coefficient B_α from the deformed to the spherical basis, $|\alpha\Omega_\alpha >= \sum_a B_a^\alpha \; |a\Omega_\alpha >$, the pairing potential Δ_p is calculated as

$$\Delta_{\alpha p\bar{\alpha}p} = -\frac{1}{2}\frac{1}{(2j_a+1)^{1/2}}\sum_{J,c} g^p_{pair} F^{J0}_{\alpha a\alpha a} F^{J0}_{\gamma c\gamma c}$$

$$\times G(aacc,J)(2j_c+1)^{1/2}(u^*_{1p_c}v_{1p_c}+u^*_{2p_c}v_{2p_c}) \; , \quad (1)$$

where $F^{JK'}_{\alpha a\bar{\beta}b} = B^\alpha_a \; B^\beta_b \; C^{JK'}_{j_\alpha\Omega_\alpha j_\beta\Omega_\beta} (K' = \Omega_\alpha + \Omega_\beta)$ is in-

---

*ejha@ssu.ac.kr
†cheoun@ssu.ac.kr

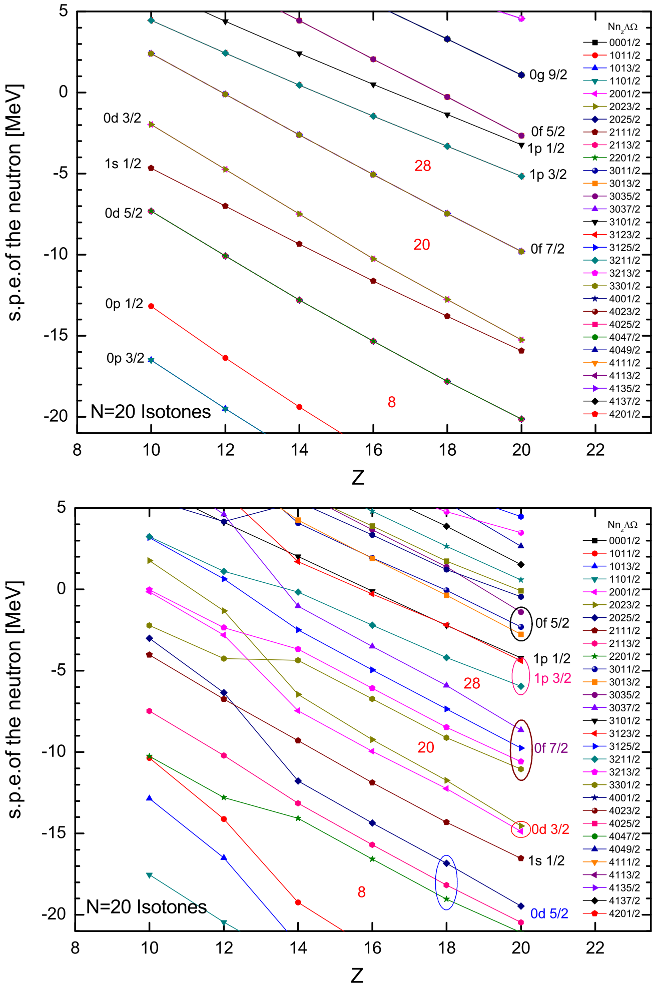

FIG. 1: (Color online) Neutron single particle energies of N=20 isotones as a function of the proton number with the deformation parameter β_2 from the relativistic mean field (RMF) (upper panel) and from B(E2) [17, 19] (lower panel) .

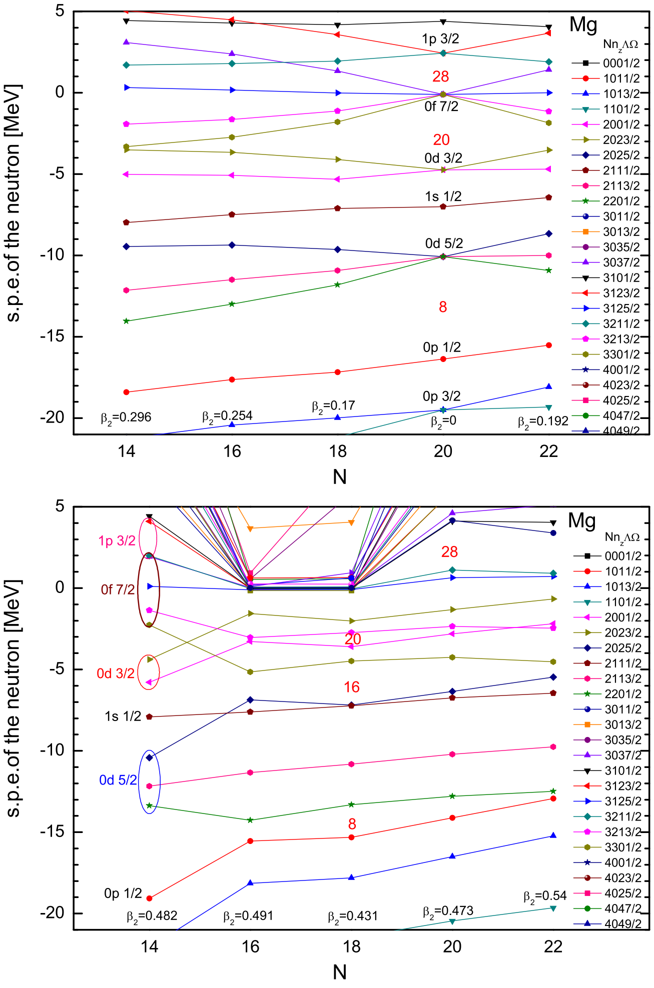

FIG. 2: (Color online) Neutron single particle energies of Mg isotopes as a function of the neutron number with the deformation parameter β_2 from the relativistic mean field (RMF) (upper panel). In lower panel, the deformation parameter β_2^{emp} for ^{26}Mg $\sim^{32}$Mg and ^{34}Mg are from the B(E2) data in Refs. [19] and [18], respectively.

troduced for the transformation to the deformed basis of G-matrix. Here K', which is a projection number of the total angular momentum J onto the z axis, is selected $K' = 0$ at the BCS stage because we consider the pairings of the quasi-particles at α and $\bar{\alpha}$ states. In order to renormalize the G-matrix, strength parameters, g^p_{pair}, g^n_{pair} and g^{pn}_{pair} are multiplied to the G-matrix [13].

The $\beta^\pm$ transition amplitudes from the ground state of an initial nucleus to the excited state are expressed by

$$\begin{aligned} &< 1(K), m|\hat{\beta}^-_K|\ QRPA > \\ &= \sum_{\alpha\alpha''\rho_\alpha\beta\beta''\rho_\beta} \mathcal{N}_{\alpha\alpha''\rho_\alpha\beta\beta''\rho_\beta} < \alpha\alpha'' p\rho_\alpha|\sigma_K|\beta\beta'' n\rho_\beta > \\ &\times[u_{p\alpha\alpha''}v_{n\beta\beta''}X_{\alpha\alpha''\beta\beta'',K} + v_{p\alpha\alpha''}u_{n\beta\beta''}Y_{\alpha\alpha''\beta\beta'',K}] \quad (2) \end{aligned}$$

where $\mathcal{N}$ is the nomalization factor and $|\ QRPA >$ denotes the correlated QRPA ground state in the intrinsic frame.

To compare to the experimental data, the GT($\pm$) strength functions

$$B^\pm_{GT}(m) = \sum_{K=0,\pm1} |< 1(K), m||\hat{\beta}^\pm_K||\ QRPA >|^2 \quad (3)$$

and their running sums $S^\pm_{GT} = \Sigma_m B^\pm_{GT}(m)$ are evaluated. The single particle states are used up to $4\hbar\omega$ in the spherical limit. Since the GT strength distributions turn out to be sensitive on the deformation parameter, β_2 [15], we took β_2 values from both the relativistic mean field (RMF)[16] and the empirical data, $\beta_2 = (4\pi/3ZR_0^2)[B(E2\uparrow)/e^2]^{1/2}(R_0 = 1.2A^{1/3})$[17–19].

In order to compare our single particle state energies (SPSEs) of N = 20 nuclei to those by other nuclear models, which show the shell evolution, we plotted SPSEs in Figs. 1 and 2, whose deformation parameters are tabulated in Table I.

TABLE I: Deformation parameters β_2 of N=20 isotones from RMF [16] and B(E2)[17, 19] for N=20 isotones.

A	β_2^{RMF}	β_2^{emp}(B(E2))
^{30}Ne	0.	0.580
^{32}Mg	0.	0.473
^{34}Si	0.	0.179
^{36}S	0.	0.168
^{38}Ar	0.	0.163
^{40}Ca	0.	0.123

TABLE II: Deformation parameters β_2^{RMF} and β_2^{emp}, and empirical(theoretical) pairing gaps $\Delta_{em}^{p;n}(\Delta_{th}^{p,n})$ for Mg isotopes. The particle-particle(particle-hole) strength parameters are taken as $g_{pp} = 1.0(g_{ph} = 1.0)$.

A	β_2^{RMF}	β_2^{emp}	Δ_{em}^{p} (Δ_{th}^{p})	$\Delta_{em}^{n}(\Delta_{th}^{n})$
^{30}Mg	0.17	0.431	2.094(2.095)	1.700(1.709)
^{32}Mg	0	0.473	2.391(2.42)	1.645(1.649)
^{34}Mg	0.192	0.54	3.29(3.308)	1.895(1.912)

The level density of *fp* shell in the upper panel in Fig.1 is increased with the decrease of proton number similarly to the result of Ref. [20] which exploited HF with SkM force (see Fig. 2 at Ref. [20]) in the QRPA scheme to study the first 2^+ states in ^{32}Mg and ^{30}Ne. This trend becomes manifest if we use the empirical deformation parameter (lower panel). Of course, the level density may lead to the anomaly of the B(E2) values as shown in Ref. [18]. In particular, N=20 shell gap is explicitly broken with the decrease of proton number by the intruder of $f_{7/2}$ state below $d_{3/2}$ state. Recent calculation by the shell model (see Fig. 3 (a) at Ref. [21]) also shows such a trend, although the effect itself was smaller than ours.

In the following, we discuss the GT strength distributions in Mg isotopes, in which ^{32}Mg is thought to locate in the island inversion. In Table II, β_2^{RMF}, β_2^{emp} and relevant pairing gaps are tabulated. Changes of SPSEs by the prolate deformation are presented in Fig. 2. The most remarkable point in the lower panel, which used β_2^{emp} accounting for the large B(E2) strength, is the disappearance of the magic number N = 20 for N = 16 $\sim$ 22 nuclei.

These shell evolution phenomena by the intruder are intimately related to the following facts. The SPSEs adopted from the deformed Woods Saxon potential naturally depend on the parameter β_2. The deformation of nuclei may be conjectured to come from macroscopic phenomena, for example, the core polarization, the high spin states and so on. Microscopic reasons may be traced to the tensor force in nucleon-nucleon interaction, which is known to account for the shell evolution according to the recent shell model calculations [21, 22]. For example, T = 0, J = 1 pairing, which is associated with the $^3S_0$ tensor force, may lead to the deformation compared to the T = 1, J = 0 pairing. Therefore, the deformation parameter adopted in this work may include implicitly and effectively such effects, because the single particle states from the deformed Wood Saxon potential show strong dependence on the β_2, as shown in Figs. 1 and 2.

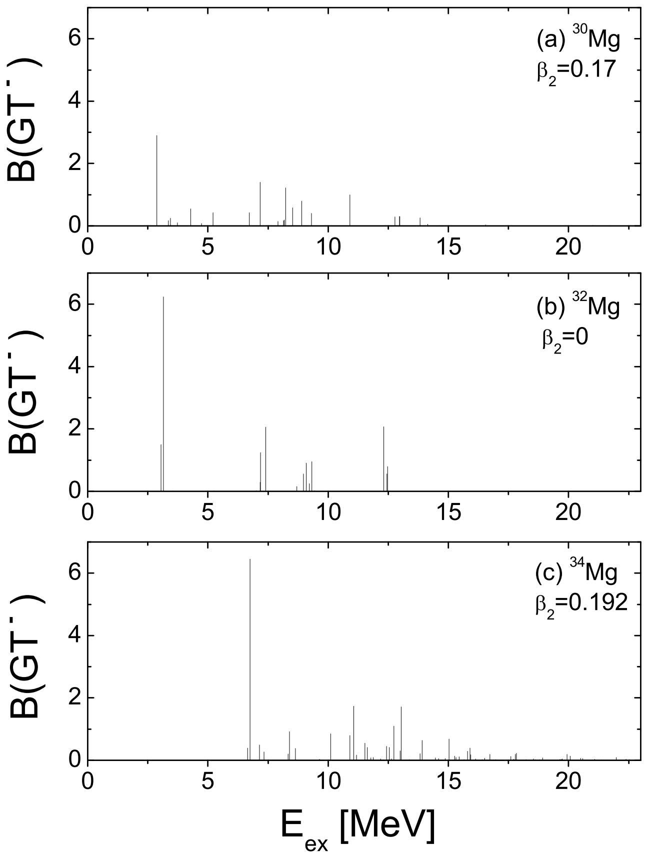

FIG. 3: (Color online) Gamow-Teller strength distribution B(GT$^-$) on Mg isotopes as a function of the excitation energy E_{ex} w.r.t. the ground state of ^{30}Mg $\sim^{34}$Mg with the deformation parameter β_2^{RMF} in the upper panel in Fig. 2.

Now we discuss the GT strengths on Mg isotopes whose SPSEs heavily depend on the neutron numbers as shown in Fig. 2. Since the nuclei considered here are expected to have large energy gaps between proton and neutron spaces, similarly to the neutron-rich nuclei of importance in the r-process, we consider only the *nn* and *pp* pairing correlation. But for the p-process nuclei, the *np* pairing could be more important than the neutron-rich nuclei because of the adjacent energy gaps of protons and neutrons. The calculations for the neutron-deficient nuclei in p-process are in progress.

In Figs.3 and 4, the GT strength distributions, B(GT$^-$), on Mg isotopes are presented as a function of the excitation energy E_{ex} w.r.t. the ground state of ^{30}Mg $\sim^{34}$Mg for β_2^{RMF} [16] and β_2^{emp} values from B(E2) data. The GT strength distributions are widely scattered into the HL states owing to the deformation. Actually, these HL GT states are intimately associated with the 2p-2h contributions which result from the wide smearing of some physical states around the Fermi surface by the

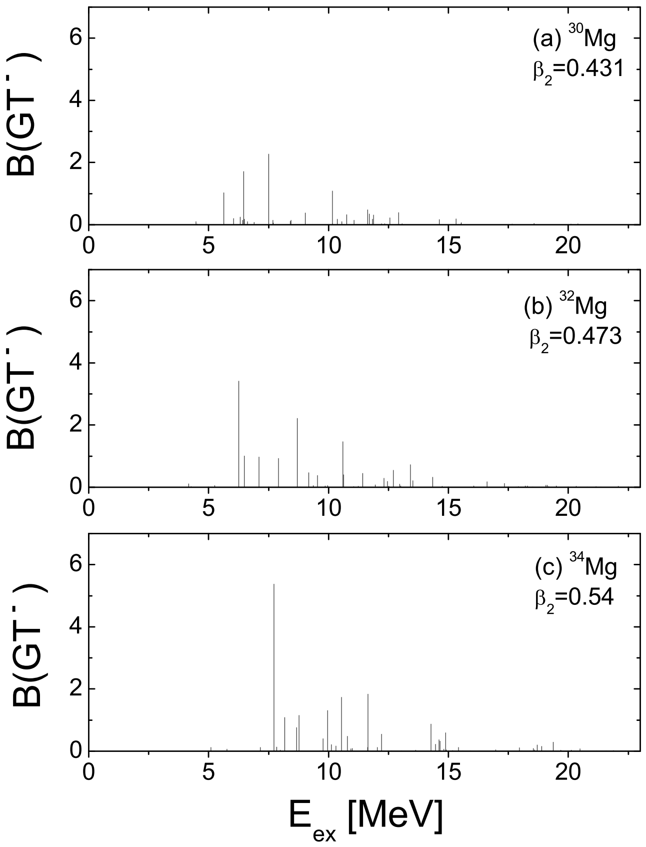

FIG. 4: (Color online) Same as Fig. 3 but with the deformation parameter β_2^{emp} in the lower panels in Fig. 2.

prolate deformation [13, 14].

One more interesting point is that some low-lying GT states disappeared if we use empirical β_2 values. This can be explained if we recollect the disappearance of the magic number $N = 20$ in Fig.2. For detailed analysis, in Fig.5, we identify main GT transitions on ^{32}Mg for $\beta_2^{emp} = 0.473$, which are the forward amplitudes X of three excitation energies having relatively larger B(GT) values in Fig.4 (b). Main transition in K = 0 comes from (2025/2) state, while major transitions in K = 1 are (2113/2)→(2111/2) and (3213/2)→(3301/2). An important point to be noticed in Fig.5 is that the (3301/2) state stemming from the $f_{7/2}$ state may contribute to the GT transition at 10.6 MeV. The (3301/2) state is generated below Fermi surface energy by the *fp*-intruder states.

In summary, to describe single particle states in deformed basis, we exploited the deformed axially symmetric Woods-Saxon potential, and performed the deformed BCS and deformed QRPA with the realistic two-body interaction recalculated in deformed basis from *ab initio* G-matrix based on Bonn potential. Results of the Gamow-Teller strength for Mg isotopes show that the deformation effect leads to a fragmentation of the GT strength into HL states and predicts the HL GT excitations to be explored by higher energy projectiles, whose excitations may affect the nuclear process in the cosmos through the GT transition. They are shown to result from the wide smearing by the increase of the Fermi surface energy due to the prolate deformation. This work was supported by the National Research Foundation of Korea (2012R1A1A3009733, 2012-009733 and 2011-0015467).

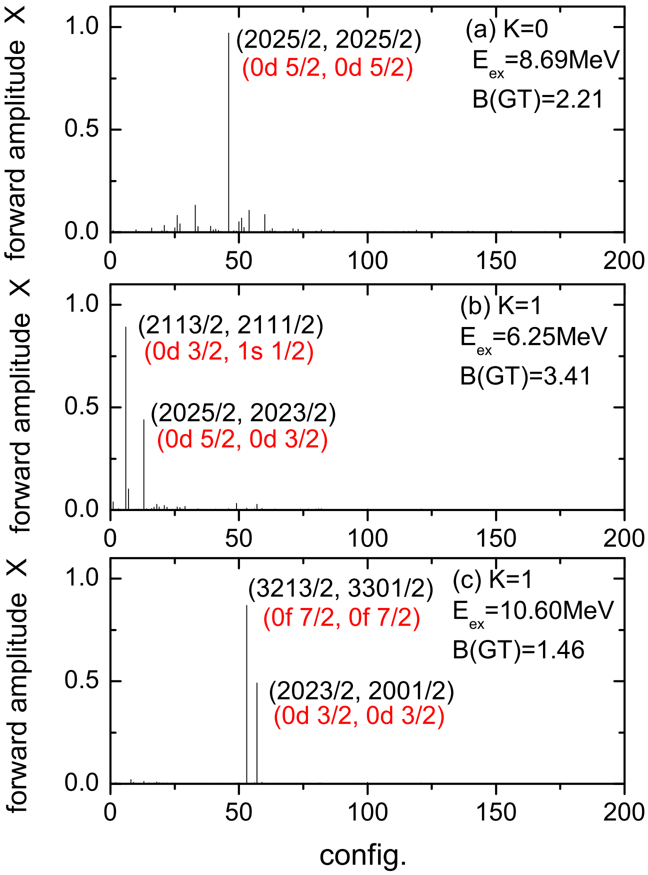

FIG. 5: (Color online) Main transitions in the forward amplitudes X for three dominant GT states w.r.t. the ground state of ^{32}Mg as a function of the configuration state for the case of Fig.4 (b).

References

[1] C. Thibault, *et al.*, Phys. Rev. C **12**, 644 (1975).
[2] G. Klotz, *et al.*, Phys. Rev. C **47**, 2502 (1993).
[3] T. Motobayashi, *et al.*, Phys. Lett. B **346**, 9-14 (1995).
[4] E. K. Warburton, *et al.*, Phys. Rev. C **41**, 1147 (1990).

[5] T. Otsuka *et al.*, Phys. Rev. Lett. **87**, 082502 (2001).
[6] T. Hayakawa, N. Iwamoto, T. Shimizu, T. Kajino, H. Umeda, and K. Nomoto, Phys. Rev. Lett. **93**, 161102 (2004).
[7] A. Heger, E. Kolbe, W.C. Haxton, K. Langanke, G. Martinez-Pinedo and S.E. Woosley, Phys. Lett. B **606**, 258 (2005).
[8] Myung-Ki Cheoun, Eunja Ha, T. Hayakawa, S. Chiba and T. Kajino, Phys. Rev. C **82**, 035504 (2010).
[9] Myung-Ki Cheoun, Eunja Ha, T. Hayakawa, Satoshi Chiba, Ko Nakamura, Toshitaka Kajino, Grant J. Mathews, arXiv:1108.4229 [nucl-th], (2011).
[10] M. Ichimura, H. Sakai, T. Wakasa, Prog. Part. Nucl. Phys. **56**, 446 (2006).
[11] F. Simkovic, L. Pacearescu, and A. Faessler, Nucl. Phys. **A733**, 321 (2004).
[12] M. S. Yousef, V. Rodin, A. Faessler, and F. Simkovic, Phys. Rev. C **79**, 014314 (2009).
[13] Eunja Ha and Myung-Ki Cheoun, arXiv:1205.4561 [nucl-th], (2012).
[14] Eunja Ha, K. S. Kim, and Myung-Ki Cheoun, arXiv:1206.2156 [nucl-th], (2012).
[15] I. Hamamoto, Phys. Rev. **C 69**, 041306(R) (2004); Phys. Rev. C **76**, 054319 (2007).
[16] G. A. Lalazissis, S. Raman, P. Ring, At. Data and Nucl. Data tables **71**, 1-40 (1999).
[17] Y. Yanagisawa *et al.*, Phys. Lett. B **566**, 84 (2003).
[18] J. A. Church, *et al.*, Phys. Rev. C **72**, 054320 (2005).
[19] S. Raman *et al.*, Atomic Data and Nuclear Data Tables **78**, 1-128(2001).
[20] M. Yamagami and Nguyen Van Giai, Phys. Rev. C **69**, 034301 (2004).
[21] T. Otsuka *et al.*, Phys. Rev. Lett. **104**, 012501 (2010).
[22] T. Otsuka *et al.*, Phys. Rev. Lett. **95**, 232502 (2005).
[23] S. G. Nilsson and I. Ragnarsson, *Shapes and Shells in Nuclear Structure* (Cambridge University Press, Cambridge, UK, 1995)